Porous structure of natural and modified clinoptilolites

Piotr Kowalczyk [a], Myroslav Sprynskyy [b,c], Artur P. Terzyk [d,*], Mariya Lebedynets [e],
Jacek Namieśnik [f], Bogusław Buszewski [b]

[a] *Department III, Institute of Physical Chemistry, Polish Academy of Sciences, Kasprzaka Str. 44/52, 01-224 Warsaw, Poland*
[b] *Department of Environmental Chemistry and Ecoanalytics, Faculty of Chemistry, Nicolaus Copernicus University, 7 Gagarina Str., 87-100 Toruń, Poland*
[c] *Department of Oil and Gas Hydrogeology, Hydrogeochemistry and Hydrosphere Protection, Institute of Geology and Geochemistry of Combustible Minerals,
Ukrainian National Academy of Sciences, 3a Naukova Str., 79053 L'viv, Ukraine*
[d] *Physicochemistry of Carbon Materials Research Group, Faculty of Chemistry, Nicolaus Copernicus University, 7 Gagarina Str., 87-100 Toruń, Poland*
[e] *Department of Ecological and Engineering Geology and Hydrogeology, Ivan Franko L'viv National University, 4 Grushevsky Str., 79005 L'viv, Ukraine*
[f] *Department of Analytical Chemistry, Chemical Faculty, Technical University of Gdańsk, 11/12 G. Narutowicza, 80-952 Gdańsk, Poland*

Abstract

The evaluation of the pore-size distribution (PSD) of natural and modified mesoporous zeolites, i.e., clinoptilolites is presented. We demonstrate the SEM results showing that the pores of fracture-type from 25–50 nm to 100 nm in size between clinoptilolite grains, as well as pores between crystal aggregates up to 500 nm in size are present in the studied material. The detailed distribution of pore sizes and tortuosity factor of the above-mentioned materials are determined from the adsorption–desorption isotherms of nitrogen measured volumetrically at 77 K. To obtain the reliable pore size distribution (PSD) of the above-mentioned materials both adsorption and desorption branches of the experimental hysteresis loop are described simultaneously by recently developed corrugated pore structure model (CPSM) of Androutsopoulos and Salmas. Evaluated pore size distributions are characterized by well-defined smooth peaks placed in the region of the mesoporosity. Moreover, the mean pore diameter calculated from the classical static measurement of nitrogen adsorption at 77 K correspond very well to the pore diameters from SEM, showing the applicability of the CPSM for characterization of the porosity of natural zeolites. We conclude that classical static adsorption measurements combined with the proper modeling of the capillary condensation/evaporation phenomena are a powerful method which can be applied for pore structure characterization of natural and modified clinoptilolites.
© 2005 Elsevier Inc. All rights reserved.

Keywords: Adsorption; Pore size distribution; CPSM model; Clinoptilolites

1. Introduction

Natural zeolites forming the corresponding group of tectosilicate mineral subclass, due to their specific crystal chemical characteristics providing the unique ion-exchange and molecular sieve properties, are known as effective adsorbents and catalysts. The zeolites are highly rigid under dehydration as well as under various aggressive surroundings actions. The molecular sieving and other physico-chemical properties of the zeolites can be managed by the thermal or chemical treatment. Such features provide the effective and wide utilization of these materials in industry, agriculture, medicine, environmental protection and other fields. About fifty natural zeolites are now known and more than one hundred and fifty have been synthesized. Synthesized analogues of the natural zeolites are usually applied in different technological processes, and the low output price conditioned by a subsurface location of massive deposits of natural zeolites throughout the world make them significantly more available for a wide utilization. Main fields of industrially important zeolite rocks are presented by clinoptilolite (rarely by mordenite, chabazite, phillipsite) tuffs and are connected with volcanic formations.

Obviously, the successful use of the clinoptilolite rocks as adsorbents or catalysts is impossible without detailed study of their porous structures as well as adsorption properties in re-

---

* Corresponding author.
E-mail address: aterzyk@chem.uni.torun.pl (A.P. Terzyk).

gard to adsorbates of different types. But the polymineral nature of these materials, existence of isomorphic mineral species of clinoptilolite, dispersion and secondary porosity pose some investigation difficulties.

Clinoptilolite being the most common natural zeolite belongs to heulandite family or structural variation of zeolite mineral group [1] and has the following general chemical formula: $(Na,K,Ca)_4Al_6Si_{30}O_{72}\cdot24H_2O$ [2]. A ratio between silicon and aluminium (Si/Al) of the clinoptilolite varies from 4.0 to 5.3 with a high thermal stability (600–800 °C). Sodium and potassium dominate mainly among sorbed exchangeable cations of clinoptilolite. The crystal structure of clinoptilolite is presented by a 3-dimensional aluminosilicate framework, whose specific building causes the developed system of micropores and channels occupied by water molecules and exchangeable cations (Na, K, Ca, Mg, Fe, Sr, Ba and others) [2,3].

The presence of two types of porosity is another interesting feature which can create some problems in the study of porous structure of clinoptilolite as well as of entire zeolite group. The primary porosity (or microporosity) is caused by the specific crystal building of zeolite mineral grains. But the secondary one is connected with sizes of zeolite and other mineral grains in the rock as well as by structural features of the rock proper. The secondary porosity is presented usually by system of meso- and macropores [2].

The porous space of non-treated natural zeolites is occupied by water molecules and exchangeable cations and this is very important for their porous structure characterization since the localization, number and sizes of cations have an influence on the pore structure. According to Tsitsishvili and co-workers [2] it is incorrect to use free channel diameters of raw zeolites for modeling their adsorption properties without study of dehydrated forms, because unit cell parameters and channel sizes change under dehydration. As adsorption properties of natural zeolites are usually managed by thermal or chemical modification, it is necessary to investigate the porous structure of their raw and modified forms.

Physical gas adsorption, electron microscopy, mercury porosimetry and XRD methods are usually used for adsorbent porous structure characterization. Electron microscopy techniques, i.e., scanning electron microscopy (SEM), transmission electron microscopy (TEM), etc., can be only used as the rough approximation for the proper estimation of the internal structure of porous materials. By using these techniques we can gather information about the shape and arrangement of the pores. Beside this, we can estimate an average geometrical pore size by simple study of a series of images.

Physical gas adsorption is an indirect method used for the investigations of the porous structure of solids. This technique is relatively fast and easy in operation. Physical adsorption of gases is often the method of first choice to study the pore characteristics of micro- and mesoporous materials and is often considered as a straightforward-to-interpret technique. This experimental technique accurately evaluates the amount of gas adsorbed on a sorbent, which is a direct measure for the porous properties and structure. The isotherm obtained from sorption measurements gives data on the surface area, pore volume and size. But some physical phenomena in micro- and mesoporous materials, being usually not accounted by models for pore size determination, may frequently lead to significant contributions in the adsorption isotherm and result in improper analysis of adsorption data [4].

In the current paper we study the pore structure of natural and modified mesoporous zeolites, i.e. clinoptilolites. We employ two experimental techniques, i.e. SEM and static volumetric adsorption–desorption measurement of nitrogen at 77 K. The SEM observations are used for the prediction of an average pore size, whereas the physical adsorption measurements with proper mathematical modeling of the adsorption–desorption phenomena are applied for the detailed estimation of the distribution of pore sizes. Since the pore structure of the considered materials consists of connected pores of different dimensions, we employed recently developed corrugated pore structure model (CPSM) [5–10]. This promising model was successfully used for the prediction of the PSDs of different kinds of materials. Since CPSM takes into account the modeling of the adsorption–desorption phenomena in the model of connected pores, the tortuosity factor can be directly determined from the empirical relationship proposed by Salmas and Androutsopoulos [7]. From our results we can conclude that natural and modified clinoptilolites are strictly mesoporous materials with pore diameter varying from 2 up to 50 nm. We show how the porosity changes during the thermal treatment and modification with HCl, and finally, we compare the obtained pore diameters with those calculated from SEM results.

2. Experimental

2.1. Initial samples

Clinoptilolite rock from Sokyrnytsya deposit (the Transcarpathian region, Ukraine) containing 70–75% clinoptilolite was used in this study. In its oxide form the formula of the Transcarpathian clinoptilolite is as follows (in %): SiO_2 to 66.7, Al_2O_3, 12.3, Fe_2O_3, 1.05, CaO, 2.10, MgO, 1.07, K_2O, 2.96, Na_2O, 2.06. Quartz, calcite, biotite, muscovite, chlorite, montmorillonite are main mineral-admixtures. Exchangeable complex of Transcarpathian clinoptilolite is presented mainly by K^+, Na^+, Ca^+ and Mg^+ ions. Thermostability of the sorbent varies from 923 to 973 K, static water-storage capacity is 9.03%, relative moisture is 10.19%, contents of exchangeable cations—53.5 meq/100 g [11,12].

The initial material was divided into fractions using mechanical sieves. Each fraction was washed up with distilled water to remove turbidity and was dried at the room temperature (air-drying). One part of the fraction 0.71–1.0 mm (HEU) was dried at the temperature of 110 °C for 4 h (HEU 110 °C) to get rid of the part of adsorbed water and the other part of the same fraction was dried at the temperature of 250 °C for 4 h (HEU 250 °C). Then the clinoptilolite samples were put in a desiccator.

2.2. Modified samples

The chemical treatment of the zeolite consisted of addition of 0.25 dm³ of the 0.1 M solutions of HCl to the samples of

clinoptilolite fraction of 0.71–1.0 mm (15 g). After 24 h the solid phases were separated from the solutions and from the Cl$^-$ ions and dried at the room temperature (HEU HCl).

2.3. Sorption measurements

Nitrogen adsorption isotherms at 77 K were measured applying ASAP 2010 (Norcross, USA) volumetric adsorption apparatus. Samples were desorbed overnight at the temperature of 200 °C under vacuum (10^{-3} Torr).

2.4. Scanning electron microscopy (SEM)

Porous structure of the clinoptilolite rock was characterized using scanning electron microscopy (SEM LEO 1430VP, England) at 1000 to 200 000 magnification with the preliminary preparation of petrographic thin sections for conservation of the unaltered crystal structure of the material.

3. Results and discussion

3.1. Theoretical basis of the CPSM

Corrugated pore structure capillary condensation/evaporation model has been recently developed by Androutsopoulos and Salmas. The detailed description of the CPSM is beyond the scope of the current study and can be found elsewhere [5–10]. In the present part of the paper we pointed out only the most important features of this approach.

The CPSM is natural improvement of the classical capillary condensation/evaporation theory proposed by Cohan [13]. It is mainly based on the random corrugated pore concept, probability principles and incorporates classical Kelvin and modified Halsey equations [14]. The pore structure is modeled as a statistically large number of independent (nonintersected) corrugated pores. Consequently the CPSM gives physical insights into adsorption/desorption equilibrium whereas the quantities characterizing dynamics of the above-mentioned processes (i.e., tortuosity factor, diffusion coefficient) can be rapidly obtained form the simulation of the adsorption/desorption phenomena. Moreover, the authors also presented the procedure for the calculation of the connectivity from the pore size distribution function closely related to the Seaton proposal [6,15,16]. The key improvement of the CPSM, beside those given above, is description of the both adsorption and desorption branch of the hysteresis loop simultaneously. As a result, only one pore size distribution response is obtained. The problem of the selection of experimental hysteresis loop branch used for the analysis of porosity is still under a heated discussion. By using non-local density functional theory, Ravikovitch and Neimark showed that when the pore-blocking (networking) effects are insignificant, both branches of the experimental hysteresis loop produce identical pore size distributions [17]. It is clear and physically justified since both hysteresis loop branches are related to the one pore size distribution. Unfortunately, the excluding of the networking effects is the main limitation of the 'independent pore model' studied by Ravikovitch et al. [18], Lastoskie et al.,

and others [19]. The assumption that the pores are not connected is highly idealized and unrealistic for some kinds of materials where the networking effects are inevitably present. Presently studied natural and modified clinoptilolites are a good example of such kind of materials.

According to the CPSM the dimensionless pore volume distribution as a function of the relative pressure varied in the range $(p/p_0)_{\min} < (p/p_0) < (p/p_0)_{\max}$ is given by [5–10]:

$$
\begin{aligned}
V_{\text{ads}}&(p/p_0) \\
&= \left[1 \bigg/ \int_{D_{\min}}^{D_{\max}} D^2 F(D)\, dD \right] \\
&\quad \times \left[4t \int_{D_h}^{D_{\max}} (D - t)F(D)\, dD + \int_{D_{\min}}^{D_c} D^2 F(D)\, dD \right. \\
&\quad + \int_{D_c}^{D_h} D^2 F(D)\, dD \left(\frac{1}{N_s} \sum_{j=1}^{j=N_s} P_j \right) \\
&\quad \left. + 4t \int_{D_c}^{D_h} (D - t)F(D)\, dD \left(\frac{1}{N_s} \sum_{j=1}^{j=N_s} (1 - P_j) \right) \right],
\end{aligned} \tag{1}
$$

whereas the relative pore space evaluated due to desorption–evaporation process is predicted by CPSM as follows [9]

$$
\begin{aligned}
V_{\text{der}}(p/p_0) &= \int_{D_h}^{D_{\max}} (D - 2t)^2 F(D)\, dD \left(\frac{2}{N_s} \frac{1 - q^{N_s}}{1 - q} - q^{N_s - 1} \right) \\
&\quad \times \left(\int_{D_{\min}}^{D_{\max}} D^2 F(D)\, dD \right)^{-1}.
\end{aligned} \tag{2}
$$

The relative saturation can be immediately obtained from Eq. (2) by simple transformation [9]

$$
V_{\text{st}}(p/p_0) = 1 - V_{\text{der}}(p/p_0). \tag{3}
$$

In the above equations the dependence of the statistical layer thickness upon nitrogen relative pressure is described by the modified Halsey t-curve [9]

$$
t\,(nm) = n \left(\frac{5}{\ln(p_0/p)} \right)^{1/3} (p/p_0)^m, \tag{4}
$$

where n, m are the empirical parameters obtained during fitting of the CPSM to the experimental data. Here it is worth to point out that Eq. (4) is very flexible and can predict the different shapes of the t-curve. For complex materials, like those considered here, Eq. (4) seems to be the most reasonable approximation since the definition of the standard reference material seems to be very difficult, from the obvious facts.

In Eq. (1) N_s denotes corrugated pore parameter and it describes the frequency of pore cross-sectional area variation along a corrugated pore configuration. Obviously, for $N_s = 2$ each segment is connected to two neighbors, i.e. the CPSM simplifies to the classical 'independent-pore' model [20]. This

parameter is very important since it describes the complexity of the internal pore structure of the investigated material. Generally, increasing N_s leads to widening of the hysteresis loop. On the other hand, this effect can be also observed by increasing heterogeneity of the investigated material (i.e., widening of the pore size distribution), so that in fact, the two above-mentioned important effects are not distinguishable.

The pore diameter D in Eqs. (1) and (2) corresponds to any intermediate geometry between the absolutely cylindrical and purely hemispherical one, i.e. $\cos(\theta) \in [0.5, 1.0]$, reads (for nitrogen at 77 K) [5]

$$D_\zeta(nm) = \frac{1.908 \cos(\theta_\zeta)}{\ln(p_0/p)} + 2t(nm). \tag{5}$$

In Eq. (5) subscript ζ conventionally denotes h—hemispherical or c—cylindrical meniscus interface geometry. However, we should take into account that these quantities are evaluated during the fitting of the theoretical models, i.e. of Eqs. (1) and (2) to the single experimental nitrogen adsorption/desorption isotherm. Consequently, the extreme cases of the interface geometry mentioned above can be more or less adequate to the investigated kind of martial.

As shown by Androutsopoulos and Salmas [5], $\cos(\theta_\zeta) < 0.5$ associated with any arbitrary geometry of the meniscus interface can be suspected for materials possessing microporosity. In fact, for many materials, especially characterized by corrugated structure, i.e., zeolites, activated carbons, etc., the assumption of the absolutely cylindrical meniscus geometry during adsorption, or purely hemispherical during desorption processes seems to be a crude approximation. Beside this, the standard Cohan equations fail for the simplest both open-ended cylindrical pores, as it was pointed out by Kruk et al. [21] and Kowalczyk et al. [22]. For these reasons the form of Eq. (5) is physically justified if the optimization process is performed correctly.

In Eqs. (1) and (2), $D_{\min}$ and $D_{\max}$ denotes the boundaries of the internal pore size distribution which is an individual feature of the investigated material. Obviously, their values are related to the relation given by Eq. (5), i.e. the beginning and the end of the experimental hysteresis loop, and the optimized meniscus interface geometry corresponding to the capillary condensation/evaporation processes. The detailed formulas for the remaining parameters closely related to the probability of the adsorption as well as desorption processes, i.e. p_j, $j = 1, 2, \ldots, N_s$ and q, can be found elsewhere [5].

Finally, for the engineering utility of the CPSM, the simple as well as flexible model representing the unknown $F(D)$—normalized pore size distribution function—should be adopted. In the current paper we applied the original Androutsopoulos and Salmas proposal, i.e. the basis consisting of the so-called 'bell-shaped' functions (see Fig. 1) [5,23]

$$F(D) = \sum_{i=1}^{M} \left[\frac{(D - D_{\min})(D - D_{\max}) \exp[b_i D]}{\int_{D_{\min}}^{D_{\max}} (D - D_{\min})(D - D_{\max}) \exp[b_i D] \, dD} \right], \tag{6}$$
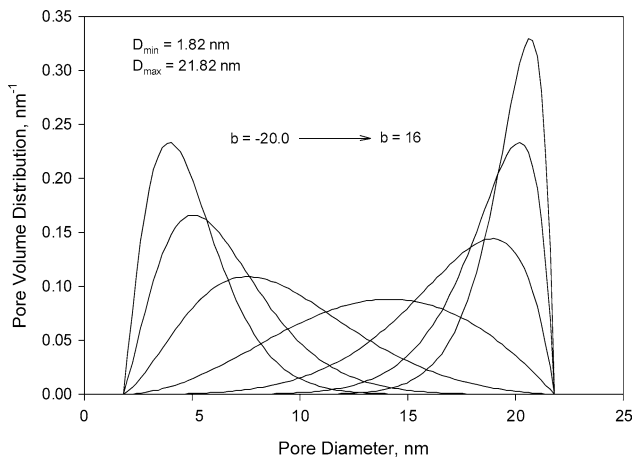

Fig. 1. Examples of the 'bell-shaped' functions used for the calculation of the pore volume distribution by the CPSM model.

where M denotes the number of the base functions (usually $M \leqslant 4$) and b_i is responsible for the ith base function shapes (see Fig. 1).

Obviously, the corresponding normalized pore volume distribution can be immediately defined as follows [5,23]

$$\begin{aligned} &F_V(D) \\ &= \sum_{i=1}^{M} \frac{D^2[(D - D_{\min})(D - D_{\max}) \exp(b_i D)]}{\int_{D_{\min}}^{D_{\max}} D^2[(D - D_{\min})(D - D_{\max}) \exp(b_i D)] \, dD}. \end{aligned} \tag{7}$$

Based on Eqs. (1)–(7), we can simulate different shapes of the hysteresis loops. This is very important for the better understanding of the novel capillary adsorption–desorption CPSM model [5].

As we mentioned above, the CPSM model gives the possibility to determine the dynamic quantities such as tortuosity factor and diffusion coefficient from static measurements. This feature is primarily important in catalysis because diffusion of compound through the pore system can determine the time of the catalytic reaction.

As proposed by Androutsopoulos and Salmas, from CPSM we can evaluate the mean pore size D_{mean}, and the effective minimum and maximum of the pore size, that is, $D_{\min,\text{eff}}$ and $D_{\max,\text{eff}}$. These parameters are used to calculate tortuosity factor τ_{CPSM} via the empirical relation [7],

$$\tau_{\text{CPSM}} = 1 + 0.69 \left(\frac{D_{\max,\text{eff}} - D_{\min,\text{eff}}}{D_{\text{mean}}} \right) (N_s - 2)^{0.58}. \tag{8}$$

The values of the $D_{\min,\text{eff}}$ and $D_{\max,\text{eff}}$ fulfill the condition [7]

$$\int_{D_{\max,\text{eff}}}^{D_{\max}} F_V(D) \, dD = \int_{D_{\min}}^{D_{\min,\text{eff}}} F_V(D) \, dD = 0.025. \tag{9}$$

At the end of this section, we presented the primary characteristics of the CPSM, i.e. incorporation of the pore networking effect. It is both quite interesting and physically justified that according to CPSM the adsorption–desorption hysteresis loop for the same pore volume distribution (PVD) strongly depends on the corrugated pore parameter N_s. As one can see from Fig. 2, increasing N_s causes the widening of the adsorption–desorption
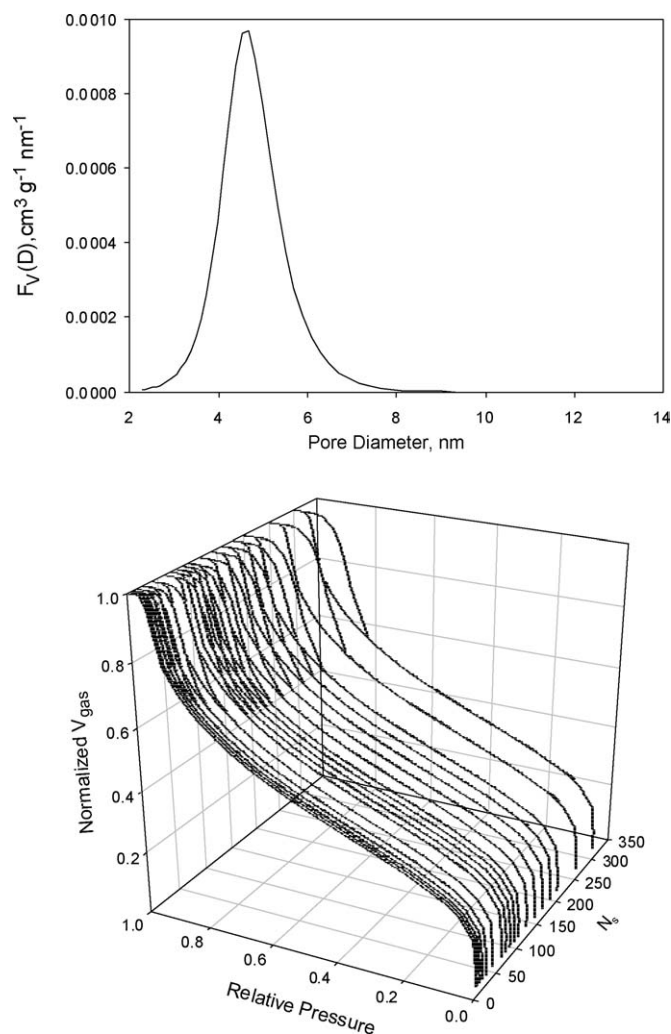
Fig. 2. Lower panel: Impact of the increasing corrugated pore parameter, N_s, on the adsorption–desorption hysteresis loops. Upper panel shows the assumed pore volume distribution. All calculations were performed for nitrogen at 77 K.

hysteresis loop whereas the PVD is kept constant. This effect cannot be observed for classical capillary condensation–evaporation models like those proposed by Barrett, Joyner, and Halenda (BJH), Dollimore and Heal (DH), etc. [24,25]. Obviously, for the materials with strong connectivity effect (i.e. characterized by the complex pore structure composed of connected pores of various sizes) N_s should increase, whereas for the materials with isolated pores (for example MCM-41, FSM-16) N_s should tend to 2.0. Our example displayed in Fig. 2 points out that for materials characterized by connected pores the standard models (mentioned above) used for estimation of PSD from nitrogen data cannot be applied. We pointed this feature of the CPSM model since the investigated materials, i.e. natural and modified zeolites, are characterized by complex structure (see Figs. 7 and 8).

3.2. Application of the CPSM model to simulate the experimental data

Figs. 3–6 present the final results obtained by means of the CPSM model. First let us pay attention for the results displayed in Fig. 3. As one can notice, the CPSM simulate the nitrogen adsorption–desorption hysteresis loop at 77 K on HEU reasonably well (see Fig. 3a). The corresponding PVD is characterized by single unsymmetrical smooth peak placed in the region of mesopores (Fig. 3b). Microporosity is absent in this sample according to volumetric nitrogen measurement data. The mean pore volume corresponding to the pore range $[D_{mean} - \delta, D_{mean} + \delta]$ is equal to 63% of the total pore volume. The region used for the calculation of the tortuosity factor is marked in Fig. 3b. For all calculations we used original combination of the simulated annealing and simple mutation algorithm [26]. As one can see from panels (c) and (d) of Fig. 3 the obtained results are stable. This fact is very important if we take into account that we optimize the function containing many independent parameters. Besides the numerical complexity in the optimization problem the obtained fitness function (i.e. accuracy of the description) and number of pore segments is very close for the independent runs of the algorithm (see panels (c) and (d) in Fig. 3). Moreover, the PVD function is unique and practically not affected by small variation of the parameters determined by fitting of the CPSM to the experimental hysteresis loop.

Figs. 4–6 present the theoretical description of the experimental nitrogen adsorption–desorption hysteresis loop at 77 K by CPSM model and corresponding PVDs. As one can see, all unmodified and modified samples of HEU are mainly composed of the pores above the pore diameter equal to 2 nm (i.e. mesopores). So, the results of the calculations are in agreement with the properties well known from the literature [27]. Microporosity is not present on PSD curves, and this feature is caused by strongly adsorbed water molecules in small pores (i.e. blocking of pores by water molecules). Therefore, according to the current computation results, nitrogen detects pores of diameter greater than 2 nm. The drying of the initial sample at the temperature of 110 °C for 4 h (HEU 110 °C) leads to desorption of the part of adsorbed water, especially from larger mesopores (see Fig. 4). This effect causes the widening and smoothing of the PVD curve, and the rise in pore volume is observed at the same time (Table 1). Further drying of the zeolite sample at the temperature of 250 °C for 4 h (HEU 250 °C) leads to decrease in porosity and the collapse of the intercrystalline porosity is observed simultaneously. The modification of the HEU by HCl acid causes a small increasing of the microporosity (i.e. about 30% of pores, see Fig. 5 and Table 1). Note that isotherm on HEU modified by HCl acid is characterized by the plateau for $0.1 \leqslant p/p_0 \leqslant 0.4$. The HEU heated in vacuum is also strictly mesoporous material characterized by a bimodal PVD. As one can observe in Fig. 6, pores tend to group into two regions, i.e. small mesopores ($D \cong 5$ nm) and larger ones ($D \cong 22$ nm).

All experimental adsorption–desorption hysteresis loops of nitrogen at 77 K on natural and modified clinoptilolites are of the type H3 according to IUPAC classification. It is well established that this type of hysteresis loop is usually given by the aggregates of platy particles or adsorbents containing slit-like pores [27]. All computed PVDs have physical meaning. First of all, both adsorption and desorption branches of the hysteresis loop are correctly predicted by the CPSM model. Next, the
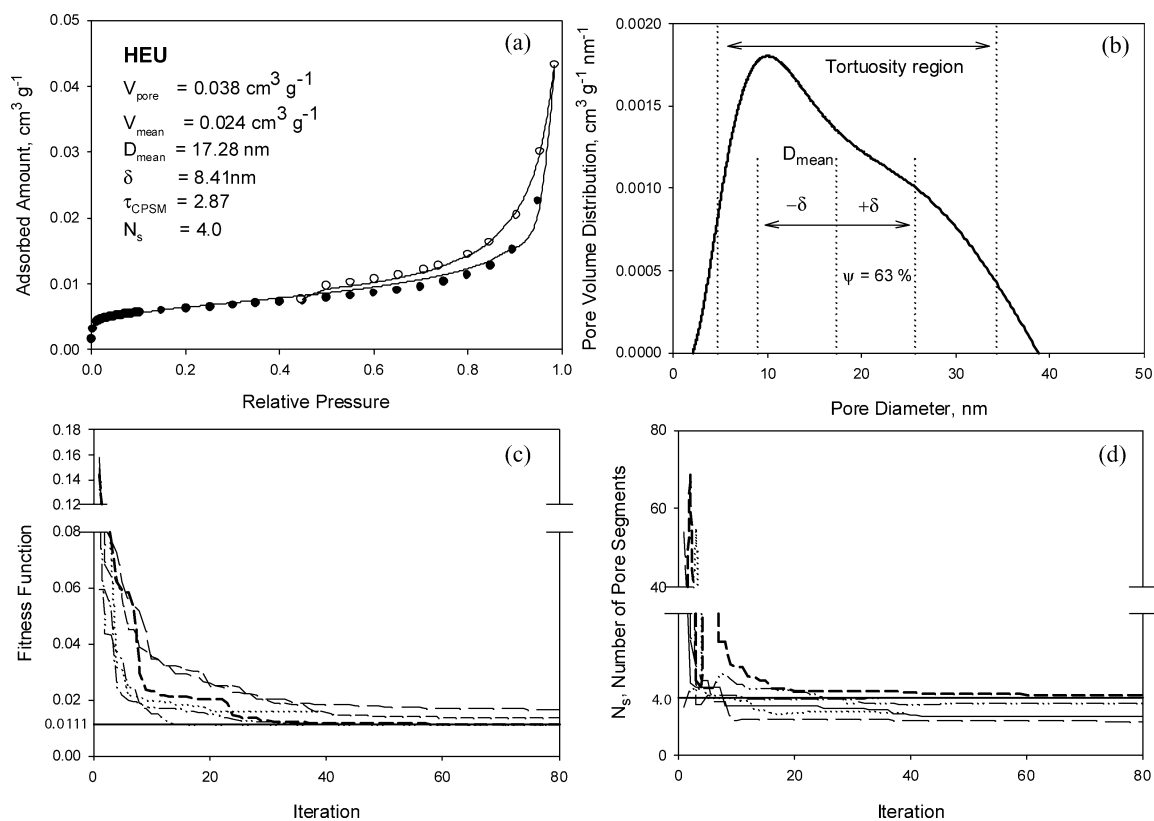
Fig. 3. Detailed analysis of the nitrogen adsorption–desorption isotherms measured at 77 K on HEU by the CPSM (a). Figure (b) presents the corresponding pore volume distributions. Figure (c) displays the accuracy of the fitting of CPSM to the experimental hysteresis loop on HEU for six independent program runs. Figure (d) shows the variation of the number of pore segments for the six independent program runs. Abbreviations: V_{pore}—total pore volume, D_{mean}—mean pore diameter, δ—standard deviation, V_{mean}—mean pore volume calculated for the pore range $[D_{\mathrm{mean}} - \delta, D_{\mathrm{mean}} + \delta]$, τ_{CPSM}—tortuosity factor, N_{s}—number of pore segments.
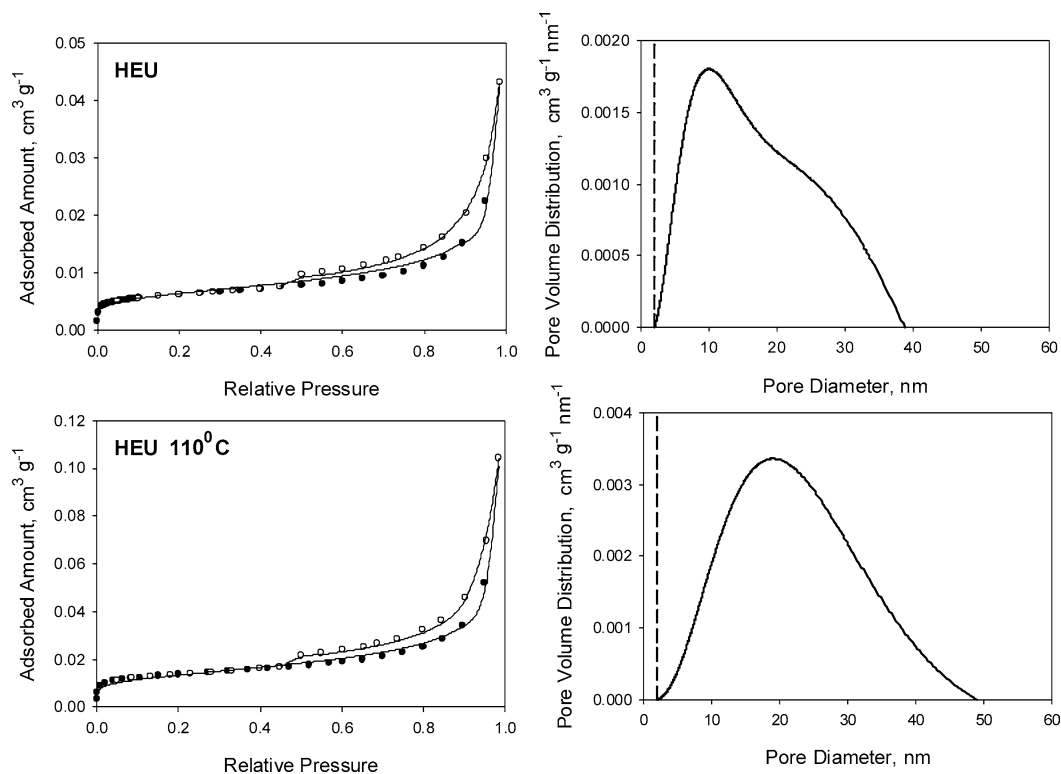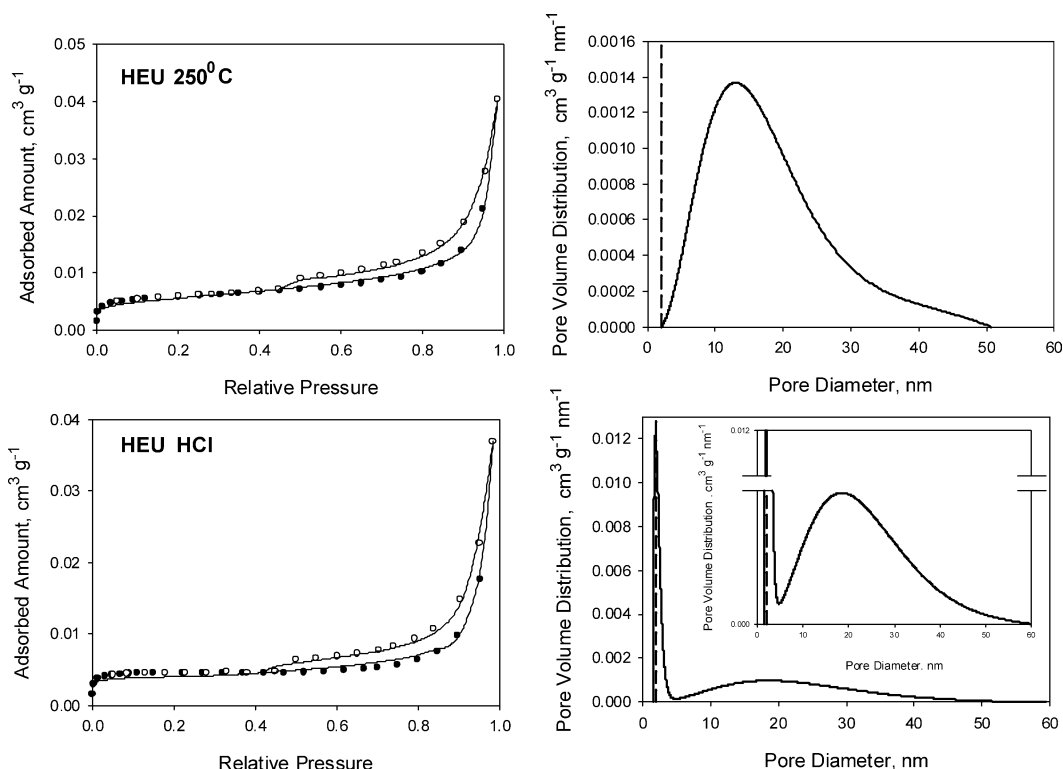

Fig. 4. Description of nitrogen adsorption–desorption isotherms measured at 77 K on HEU by the CPSM (left panel). Right panel presents the corresponding pore volume distributions (vertical dashed line shows the upper boundary for micropores). Abbreviations: HEU 110 °C indicates the heat treatment at 110 °C.

Fig. 5. Description of nitrogen adsorption–desorption isotherms measured at 77 K on HEU by the CPSM (left panel). Right panel presents the corresponding pore volume distributions (vertical dashed line shows the upper boundary for micropores). Abbreviations: HEU 250 °C indicates the heat treatment at 250 °C; HEU HCl indicates the treatment of the sample by HCl acid.
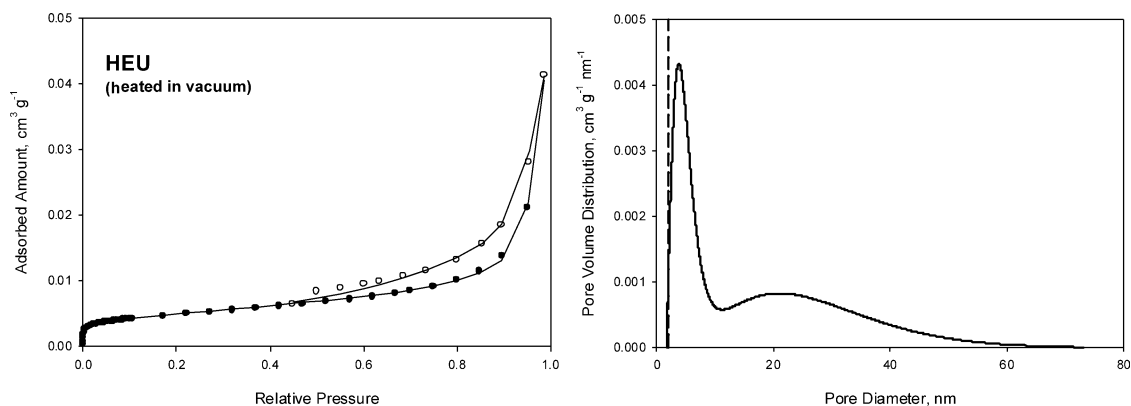

Fig. 6. Description of nitrogen adsorption–desorption isotherms measured at 77 K on HEU by the CPSM (left panel). Right panel presents the corresponding pore volume distributions (vertical dashed line shows the upper boundary for micropores). Abbreviations: HEU (heated in vacuum) indicates the heat treatment in vacuum.

PVDs are characterized by smooth peaks. Finally, the PVDs vanish on the boundaries. The computed parameters are summarized in Table 1. For all considered samples of natural and modified clinoptilolites the number of pore segments, $N_s > 2$, which confirms the SEM observation that the independent pore model in not adequate for the modeling of the PSV from the single nitrogen adsorption–desorption isotherm measured at 77 K.

3.3. SEM results

Photographs using SEM at magnification of several thousand show that the clinoptilolite rock is a fine-graining mate-

rial of lamellar texture. At dividing ability increase it may be seen that separate plates or bars (some microns in size) are not individual crystal grains of clinoptilolite, but are aggregates presented by finer grains of the mineral. Such splitting of zeolite grains is typical for clinoptilolite cleavage that is a consequence of hydrothermal solution filtration. At 20 000 magnification (Figs. 7 and 8) the diverse orientation of the separate crystalline aggregates of the zeolite is observed.

The thin-bar crystalline forms of clinoptilolite grains and their face-to-face arrangement are enough well conspicuous in the limits of each block (aggregate). But there are also blocks with domination of entirely disordered crystal orienta-

Table 1
Structural parameters calculated form adsorption–desorption isotherms of nitrogen at 77 K applying the CPSM model

Sample	HEU	HEU 110 °C	HEU 250 °C	HEU HCl	HEU (heated in vacuum)
V_{pore} (cm^3 g^{-1})	0.038	0.081	0.026	0.037	0.041
V_{mean} (cm^3 g^{-1})	0.024	0.052	0.018	0.019	0.027
D_{mean} (nm)	17.28	22.26	17.96	15.83	17.07
δ (nm)	8.41	9.01	8.90	12.82	13.92
τ_{CPSM}	2.87	2.34	2.26	2.85	3.51
N_s	4.00	3.51	2.89	3.00	3.23

Note. Abbreviations: HEU 110 °C indicates the heat treatment at 110 °C; HEU 250 °C the heat treatment at 250 °C; HEU HCl the treatment of the sample by HCl acid; HEU (heated in vacuum) the heat treatment in vacuum; V_{pore}—total pore volume, D_{mean}—mean pore diameter, δ—standard deviation, V_{mean}—mean pore volume calculated for the pore range $[D_{mean} - \delta, D_{mean} + \delta]$, τ_{CPSM}—tortuosity factor, N_s—number of pore segments.
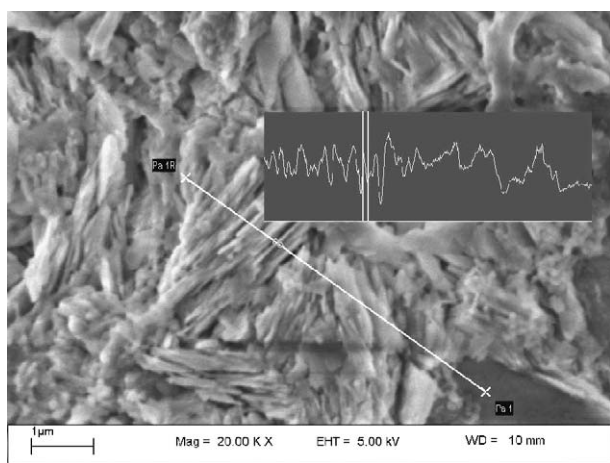

Fig. 7. The soldered fine- or latent-crystalline structure of the Sokyrnytsya clinoptilolite tuff studied by the SEM (at 20 000 magnification).
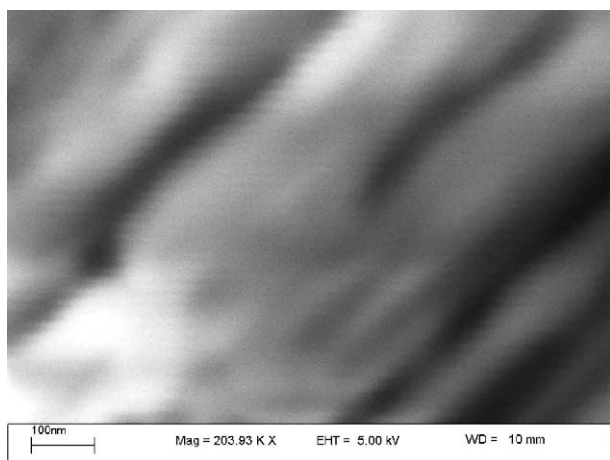

Fig. 8. The soldered fine- or latent-crystalline structure of the Sokyrnytsya clinoptilolite tuff studied by the SEM (at 200 000 magnification).

tion. Clinoptilolite grains are flat, long in 010 axis bars. They are 40 nm thick, 300–700 nm wide, 300–1000 nm long in average. There are pores of fracture-type 25–50 nm to 100 nm in size between clinoptilolite grains as well as pores between crystal aggregates up to 500 nm in size. The observed profiles of the

thin sections' surfaces demonstrate that even the finest grains are characterized by cleavage with separate bar of 20 nm in size. Hence the clinoptilolite form Sokyrnytsya field has a latent fine-crystalline structure with the crystal size of $40 \times 500 \times 700$ nm in average. Geometrical specific area of the grains is near 30 m^2 per gram of the zeolite. Generally intergrain fractures correspond to mesopores with sizes 25–50 nm.

4. Conclusions

It is shown that the developed recently CPSM model can be successfully applied for the calculation of the porosity of natural zeolites. Applying this model we provide full characteristics of natural and modified mesoporous zeolites, i.e. clinoptilolites, and discuss the changes due to thermal treatment and modification with HCl. We show that the obtained pore diameters cover the range determined from the SEM results. Thus this method of porosity calculation is probably one of the most advanced and reliable ones.

Acknowledgments

References

[1] D.W. Breck, Zeolite Molecular Sieves, Wiley–Interscience, New York, 1974.
[2] G. Tsitsishvili, T. Andronikashvili, G. Kirov, L. Filizova, Natural Zeolites, Ellis Horwood, New York, 1992.
[3] F.A. Mumpton, Am. Mineral. 45 (1960) 351.
[4] J.C. Groen, L.A.A. Peffer, J. Perez-Ramirez, Micropor. Mesopor. Mater. 60 (2003) 1.
[5] G.P. Androutsopoulos, C.E. Salmas, Ind. Eng. Chem. Res. 39 (2000) 3747; G.P. Androutsopoulos, C.E. Salmas, Ind. Eng. Chem. Res. 39 (2000) 3764.
[6] G.S. Armatas, C.E. Salmas, M. Louloudi, G.P. Androutsopoulos, P.J. Pomonis, Langmuir 19 (2003) 3128.
[7] C.E. Salmas, G.P. Androutsopoulos, Ind. Eng. Chem. Res. 40 (2001) 721.
[8] C.E. Salmas, A.K. Ladavos, S.P. Skaribas, P.J. Pomonis, G.P. Androutsopoulos, Langmuir 19 (2003) 8777.
[9] C.E. Salmas, V.N. Stathopoulos, P.J. Pomonis, G.P. Androutsopoulos, Langmuir 18 (2002) 423.
[10] C.E. Salmas, V.N. Stathopoulos, P.J. Pomonis, H. Rahiala, J.B. Rosenholm, G.P. Androutsopoulos, Appl. Catal. A 216 (2001) 23.
[11] G.R. Bulka, V.M. Vinokurov, V.V. Vlasov, Clinoptilolite, Metsniereba, Tbilisi, 1977 (in Russian).
[12] F.D. Ovcharenko, N.Ye. Shcherbatyuk, Yu.I. Tarasevich, V.A. Suprychyov, Clinoptilolite, Mentsniereba, Tbilisi, 1977 (in Russian).
[13] L.H. Cohan, J. Am. Chem. Soc. 60 (1938) 433; L.H. Cohan, J. Am. Chem. Soc. 66 (1940) 98.
[14] G. Halsey, J. Chem. Phys. 16 (1948) 931.
[15] N.A. Seaton, Chem. Eng. Sci. 46 (1991) 1895.
[16] H. Liu, L. Zhang, N.A. Seaton, J. Colloid Interface Sci. 156 (1993) 285.
[17] P.I. Ravikovitch, V.N. Neimark, Stud. Surf. Sci. Catal. 129 (2000) 597.

[18] P.I. Ravikovitch, A. Vishnyakov, R. Russo, A.V. Neimark, Langmuir 16 (2000) 2311.

[19] C. Lastoskie, N. Quirke, K.E. Gubbins, in: W. Rudzinski, W.A. Steele, G. Zgrablich (Eds.), Equilibria and Dynamics of Gas Adsorption on Heterogeneous Solid Surfaces, Elsevier, Amsterdam, 1997.

[20] D.D. Do, Adsorption Analysis: Equilibria and Kinetics, Imperial College Press, Singapore, 1998.

[21] M. Kruk, M. Jaroniec, A. Sayari, Langmuir 13 (1997) 6267.

[22] P. Kowalczyk, M. Jaroniec, A.P. Terzyk, K. Kaneko, D.D. Do, Langmuir 21 (2005) 1827.

[23] P. Kowalczyk, Theoretical Evaluation of Surface Nanostructures with Gas Adsorption, Chiba University Press, Chiba, 2004.

[24] E.P. Barrett, L.G. Joyner, P.P. Halenda, J. Phys. Chem. 73 (1951) 373.

[25] D. Dollimore, G.R. Heal, J. Appl. Chem. 14 (1964) 109.

[26] Z. Michalewicz, Genetic Algorithms + Data Structures = Evolution Programs, WNT, Warsaw, 1999 (in Polish).

[27] F. Rouquerol, J. Rouquerol, K. Sing, Adsorption by Powders and Porous Solids. Principles, Methodology and Applications, Academic Press, London, 1999.